

# Degradation of tiamulin by a packed bed dielectric barrier plasma combined with TiO<sub>2</sub> catalyst

Kun YANG (杨坤)<sup>1,2</sup>, Hongwei SHEN (沈红伟)<sup>1,2</sup>, Yueyue LIU (刘月月)<sup>1,2</sup>,  
Yang LIU (刘阳)<sup>1,2</sup>, Pingji GE (葛平基)<sup>1,2</sup> and Dezheng YANG (杨德正)<sup>2,3,\*</sup>

<sup>1</sup> School of Science, Shihezi University, Shihezi 832003, People's Republic of China

<sup>2</sup> Key Laboratory of Environmental Monitoring and Pollutant Control of Xinjiang Bingtuan, Shihezi University, Shihezi 832003, People's Republic of China

<sup>3</sup> Key Lab of Materials Modification, Dalian University of Technology, Ministry of Education, Dalian 116024, People's Republic of China

E-mail: [yangdz@dlut.edu.cn](mailto:yangdz@dlut.edu.cn)

Received 3 December 2021, revised 30 April 2022

Accepted for publication 5 May 2022

Published 27 July 2022



## Abstract

Recently, a plasma catalyst was employed to efficiently degrade antibiotic residues in the environment. In this study, the plasma generated in a packed bed dielectric barrier reactor combined with TiO<sub>2</sub> catalyst is used to degrade the antibiotic tiamulin (TIA) loaded on the surface of simulated soil particles. The effects of applied voltage, composition of the working gas, gas flow rate and presence or absence of catalyst on the degradation effect were studied. It was found that plasma and catalyst can produce a synergistic effect under optimal conditions (applied voltage 25 kV, oxygen ratio 1%, gas flow rate 0.6 l min<sup>-1</sup>, treatment time 5 min). The degradation efficiency of the plasma combined with catalyst can reach 78.6%, which is 18.4% higher than that of plasma without catalyst. When the applied voltage is 30 kV, the gas flow rate is 1 l min<sup>-1</sup>, the oxygen ratio is 1% and the plasma combined with TiO<sub>2</sub> catalyst treats the sample for 5 min the degradation efficiency of TIA reached 97%. It can be concluded that a higher applied voltage and longer processing times not only lead to more degradation but also result in a lower energy efficiency. Decreasing the oxygen ratio and gas flow rate could improve the degradation efficiency. The relative distribution and identity of the major TIA degradation product generated was determined by high-performance liquid chromatography–mass spectrometry analysis. The mechanism of TIA removal by plasma and TiO<sub>2</sub> catalyst was analyzed, and the possible degradation path is discussed.

**Keywords:** packed bed dielectric barrier discharge, plasma catalyst, tiamulin (TIA) antibiotics degradation, degradation mechanism

(Some figures may appear in colour only in the online journal)

## 1. Introduction

Antibiotics are widely used in livestock and aquaculture due to their efficacy in preventing and treating diseases caused by bacteria. However, environmental scientists have recently found

recognized antibiotic residues as important emerging environmental pollutants, with the development of antibiotic resistance having adverse effects on ecology and human health [1]. Therefore, from the perspective of environmental protection and human health, it is particularly important to remove antibiotic residues efficiently from soil [2]. Recently, a variety of methods have been explored to mitigate environmental contamination by

\* Author to whom any correspondence should be addressed.

antibiotics, such as adsorption, catalytic degradation, biodegradation, photocatalytic degradation and advanced oxidation [3]. These different approaches each have their own advantages and challenges.

Non-thermal plasmas (NTPs), which can produce active substances such as electrons, highly excited atoms, ions, radicals, molecules, shock waves and ultraviolet (UV) light, could be promising for removing pollutants [4]. As an environmentally friendly and efficient technology, plasma technology can be used in treating organic pollutants, remediating wastewater, reducing exhaust gas emission and treating solid waste [5]. Kim *et al* used a dielectric barrier discharge (DBD) plasma to degrade antibiotics in synthetic wastewater, and their results show that this technology can play an important role in the treatment of organic pollutants [6].

In recent years, plasma combined with catalyst has shown synergistic effects, effectively improving the efficiency of antibiotic degradation. Guo *et al* used a pulsed discharge plasma (PDP) to induce  $\text{WO}_3$  to co-degrade cyclic propylene satin (CIP) in water. After 60 min of processing,  $0.16 \text{ g l}^{-1}$   $\text{WO}_3$  increased the CIP removal rate from 71.3% to 99.6% [7]. Aziz *et al* studied the degradation of the drugs dichloro-fenac acid and ibuprofen in aqueous solutions by ozone, photocatalytic and non-thermal plasma. They found that the synergy of several methods greatly improved the efficiency of drug degradation [8]. He *et al* studied the significant synergistic effect of nano- $\text{TiO}_2$  and corona discharge plasma in the degradation of tetracycline in aqueous solutions [9]. The packed bed method in DBD is also a major method that researchers often use to degrade organic pollutants [10, 11]. Ma and Xu studied the degradation and kinetics of reaction of typical organophosphorus pesticides in a packed bed reactor. The degradation efficiency was 80% at 35 kV with a gas flow rate of  $800 \text{ ml min}^{-1}$  and initial concentration of  $11.2 \text{ mg l}^{-1}$  [12]. The results of previous studies have demonstrated that the efficiency of degradation of antibiotic residues can be improved by increasing the discharge voltage, frequency, thickness of the catalyst bed, etc.

Tiamulin (TIA) is an antibiotic widely used in pig breeding, and existing studies have shown that TIA in pig excrement will enter the soil and surface water along with excrement used as fertilizer, which will lead to the risk of resistance in the environment [13]. In this study, plasma generated by the discharge of a packed bed dielectric barrier reactor (PBR) driven by an AC power supply degrades solid-phase TIA in combination with a catalyst. We have optimized the experimental parameters of degradation and derived the most likely path of TIA degradation. All the other operating parameters of the PBR plasma setup were kept fixed, such as the electrode gap, catalyst bed thickness and catalyst particle diameter; the treatment time, applied voltage, gas flow rate, working gas composition and catalyst whose effects on the degradation will be studied were varied. The mechanism and pathway of degradation were also analyzed.

## 2. Experiment

### 2.1. Experimental setup and apparatus

A schematic of the experimental setup used to degrade solid-phase TIA is pictured in figure 1(a). It is designed for gas–solid discharge and the overall system comprises four parts: the power supply system, the gas delivery system, the PBR and the analytical system. The peak voltage of the AC voltage source (CTP-2000P, Nanjing Suman Electronics Co. Ltd) with a center frequency of 14 kHz can be adjusted in the range of 0–35 kV. The flow rates of nitrogen and oxygen were controlled by two mass flow controllers (MFCs) to adjust the ratio of gas components. As shown in figure 1(a), the diagnostic system consisted of two main components: electric and optical diagnosis. A voltage probe (P6015A, Tektronix, 75 MHz bandwidth) and current probe (TCP312, Tektronix, 100 MHz bandwidth) are used to measure the applied voltage ( $V_d$ ) and discharge current ( $I_d$ ) profiles, respectively. All the wave-forms are recorded by an oscilloscope (TDS5054B, Tektronix, 500 MHz bandwidth). The longitudinally adjustable fiber head is parallel to the surface of the electrode. The emission spectrometer (F-4500, Hitachi) that captures the optical emission from the discharge region transmitted through the optical fiber is a three-channel spectrometer that uses a grating as a beam splitter and a CCD array as a detector. It can measure wavelengths from 300–800 nm at 0.1 nm optical resolution. The concentrations of TIA during plasma treatment were assessed by UV–visible spectrophotometer (Cary 6000, Agilent, USA) in the wavelength range of 190–900 nm.

A PBR with a DBD was designed to investigate the effects of PBR treatment on degradation of TIA (figure 1(b)). The PBR consists of two coaxial layers of quartz tubes with inner and outer layers having an inside diameter of 4 mm and outside diameter of 15 mm and a length of 200 mm. The  $\gamma\text{-Al}_2\text{O}_3$  pellets loaded with TIA are placed in the middle of the two layers of quartz tubes. The discharge in this area forms the plasma of the dielectric barrier. A copper bar with a diameter of 3 mm used as the high-voltage electrode was inserted into the inner quartz tube by rubber plug fittings. The grounded electrodes comprised an iron net with winding length of 100 mm installed outside the outer quartz tube surface. The gas supply was administered through a gas inlet followed by gas ionization utilizing an electric field between two electrodes. The plasma produced by the discharge acts on the surface of the filler.

### 2.2. Material preparation

Solid-phase TIA was obtained from Zhejiang University Sunny Technology (Xinjiang, China). The initial concentration of TIA in the solution was measured before adsorption. The  $\gamma\text{-Al}_2\text{O}_3$  particles were then immersed and adsorbed for 20 min, then taken out and dried overnight. Two samples were prepared under the same conditions, one group was kept as a control and the other group was treated with plasma. In addition, the  $\gamma\text{-Al}_2\text{O}_3$  particles loaded with  $\text{TiO}_2$  were

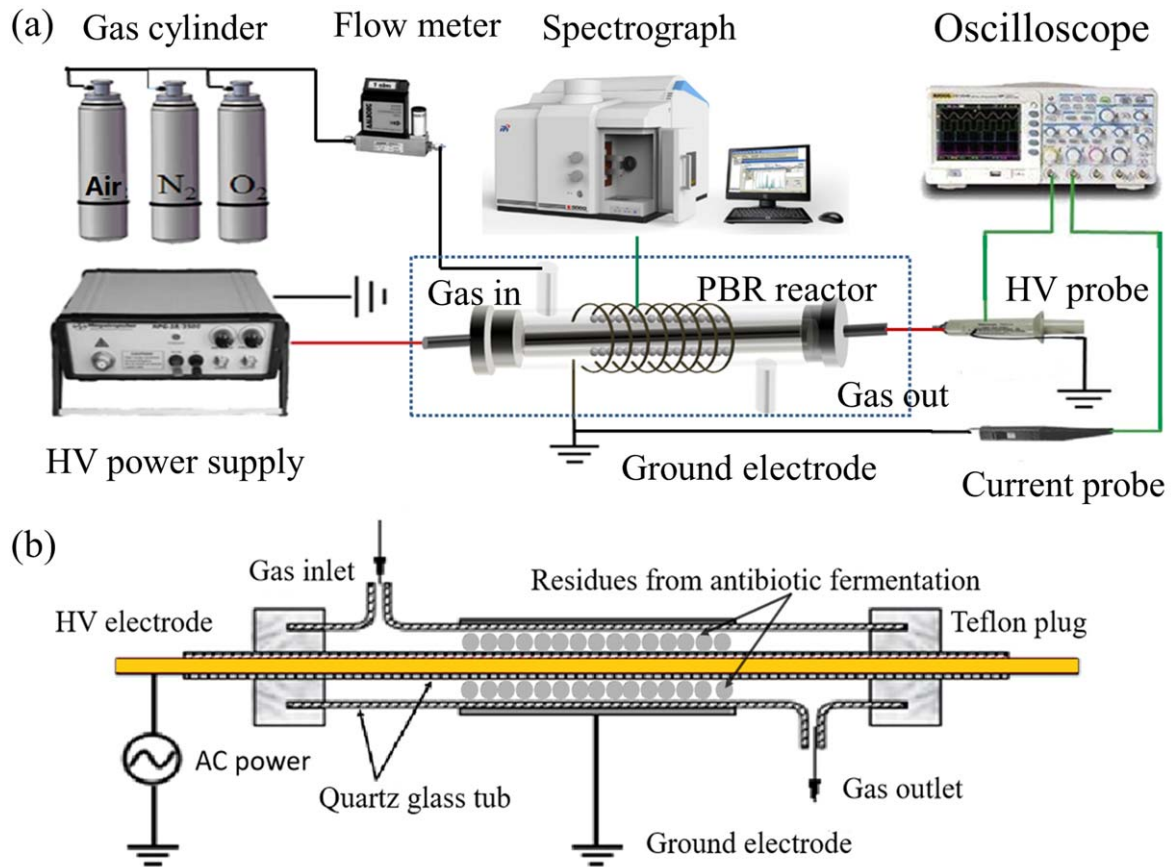


**Figure 1.** (a) Schematic diagram of the experimental apparatus for degradation of TIA and (b) schematic illustration of the structure of the PBR.

prepared by a gel method, which supported TIA in the same way as described above.

### 2.3. Measurement

All the experiments were carried out at room temperature and ambient pressure. The efficiency of TIA degradation was calculated as follows:

$$\eta = \frac{C_0 - C_t}{C_0} \% \quad (1)$$

where  $C_0$  refers to the initial concentration ( $\text{mg l}^{-1}$ ) and  $C_t$  is the concentration of TIA at a given reaction time.

The Lissajous method was used to determine the power consumption. The total power consumption of the reactor is proportional to the area of the Lissajous diagram and can be calculated as [14]

$$P = fC_m A \quad (2)$$

where  $C_m$  is the measuring capacitance ( $\mu\text{F}$ ),  $f$  is the frequency of alternating current (Hz) and  $A$  is the area of the Lissajous diagram.

The average discharge power and the energy efficiency of TIA degradation are calculated with the following equation:

$$G = \frac{m_{\text{TIA}}}{Pt} \quad (3)$$

where  $m_{\text{TIA}}$  is the quantity of TIA removed,  $P$  is the discharge power (W) and  $t$  is the discharge time (s).

The kinetic analysis of TIA degradation is carried out following first-order kinetic model, which is shown as follows:

$$\ln\left(\frac{C_0}{C_t}\right) = kt \quad (4)$$

where  $C_0$  and  $C_t$  have the same definition as equation (1),  $k$  is the kinetic constant and  $t$  is the reaction time (s).

## 3. Results and discussion

### 3.1. Plasma characteristics of the PBR

Figure 2 shows the discharge images in the PBR captured by a camera (Canon 5D mark IV, 500 ms exposure time) in the applied voltage range from 18 to 25 kV, with a gas flow rate of  $1 \text{ l min}^{-1}$ , a discharge frequency of 14 kHz and an oxygen ratio of 1%. It is seen that microdischarge starts to occur after the appearance of the breakdown voltage. The uniform dispersion discharge can be seen in the photos. When the voltage is sufficiently high ( $>20 \text{ kV}$ ), a discharge with intense light emission begins in the electrode gap. The voltage–current characteristics confirm that the breakdown of gas in the DBD results in many current filaments called micro-discharges,

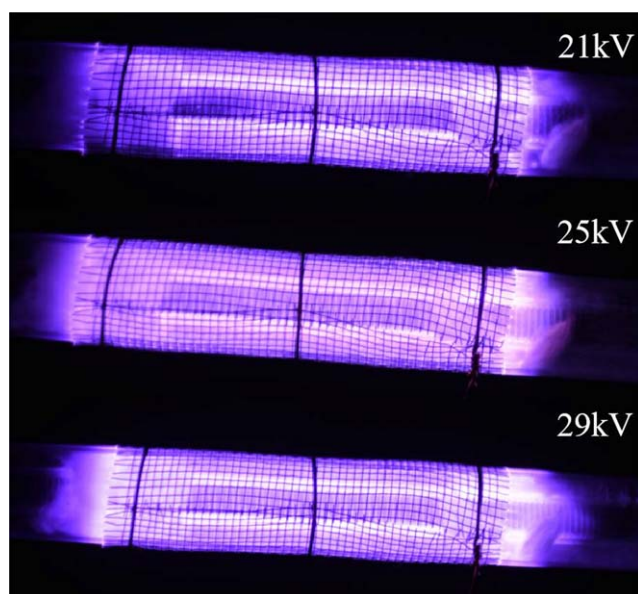


Figure 2. Discharge image of the PBR.

which agrees with the image of the discharge in figure 2. The duration of the current filaments is  $20\ \mu\text{s}$  and the amplitude is  $25\ \text{mA}$ . This shows that the discharge in the PBR is still in filamentous discharge mode. This indicates that the energy transfer in each cycle is a sine function, the equivalent voltage and current per delivery can be integrated by the area of the region of corresponding state variables, and the input discharge power can be calculated from the latent relationship [15]. The discharge current filaments can be clearly observed when the discharge gap is broken down at  $21\ \text{kV}$ . The filament current with an amplitude of about  $7\ \text{mA}$  overlaps the displacement current. The duration of the discharge is about  $30\ \mu\text{s}$  in each half period. In this condition, the discharge is in filament discharge mode. The discharge current shows significant changes at  $25\ \text{kV}$ . Figure 3 illustrates the corresponding wave-forms of applied voltage and discharge current at a driving frequency of  $14\ \text{kHz}$ . From figure 3, the wave-forms of the discharge current and voltage illustrate the production of a large number of diffusive discharges in the discharge images. Improvement of discharge homogeneity enables the discharge to be evenly distributed in the discharge gaps and avoids the situation where most of the discharge area is not filled by plasma due to the uneven discharge in the filament mode. The stable and homogeneous discharge generated in the PBR is vital to the degradation of TIA, with obvious merits for enhancing degradation efficiency and energy efficiency, and has significant application prospects for soil remediation.

### 3.2. Selection of the initial concentration

In the early stage of this experiment, the adsorption concentration was detected as follows: with ultrapure water as the solvent,  $20\ \text{ml}$  TIA solutions with initial concentrations of  $2\ \text{g l}^{-1}$ ,  $4\ \text{g l}^{-1}$ ,  $6\ \text{g l}^{-1}$ ,  $8\ \text{g l}^{-1}$  and  $10\ \text{g l}^{-1}$  were prepared. Five pieces of  $\gamma\text{-Al}_2\text{O}_3$  pellets with a mass of  $10\ \text{g}$  (average particle size  $1\ \text{mm}$ ) were placed into each initial solution to soak for  $20\ \text{min}$  for adsorption of TIA. The  $\gamma\text{-Al}_2\text{O}_3$  pellets were

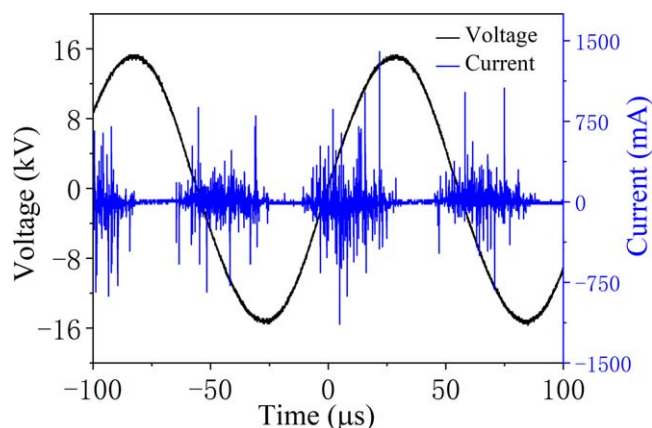


Figure 3. Typical wave-forms of applied voltage ( $U_t$ ) and current ( $I_t$ ).

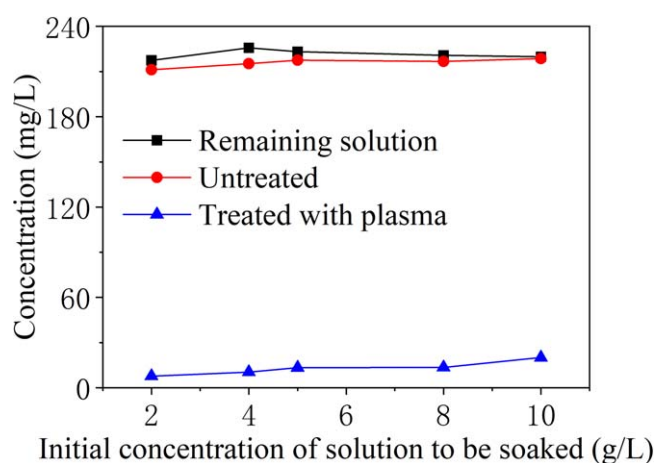


Figure 4. Adsorption and desorption experiments for  $\gamma\text{-Al}_2\text{O}_3$  particles in different concentrations of TIA solution.

drained and placed in an oven set at  $80\ ^\circ\text{C}$  for  $10\ \text{h}$ . After that, the pellets were put into  $20\ \text{ml}$  of ultrapure water for  $30\ \text{min}$  ultrasonic treatment and  $10\ \text{min}$  centrifugation ( $9000\ \text{rpm}$ ) for desorption. The supernatant in the centrifuge tube was removed, and its absorbance at  $205\ \text{nm}$  was measured with a UV spectrophotometer. The concentration can be determined by comparison with the standard curve for aqueous solutions of TIA.

Figure 4 compares the concentration of the remaining solution after the addition of adsorbing particles to TIA solutions with different initial concentrations and the concentration of the desorbed solution before and after the particles were subjected to plasma discharge treatment. The concentration of the remaining solution after adsorption is close to the concentration after adsorption of TIA but not subject to plasma discharge. But after discharge treatment, the concentration is greatly reduced. The degradation of TIA by plasma produced by PBR is obvious. Judging from the changing trends of the three curves, the  $\gamma\text{-Al}_2\text{O}_3$  particles have reached adsorption saturation for the TIA solution with an initial concentration of  $4\ \text{g l}^{-1}$ . The initial concentration of the solution selected to soak the sample was  $4\ \text{g l}^{-1}$ , and the supernatant concentration of the sample after adsorption and desorption was  $216.163\ \text{mg l}^{-1}$ .



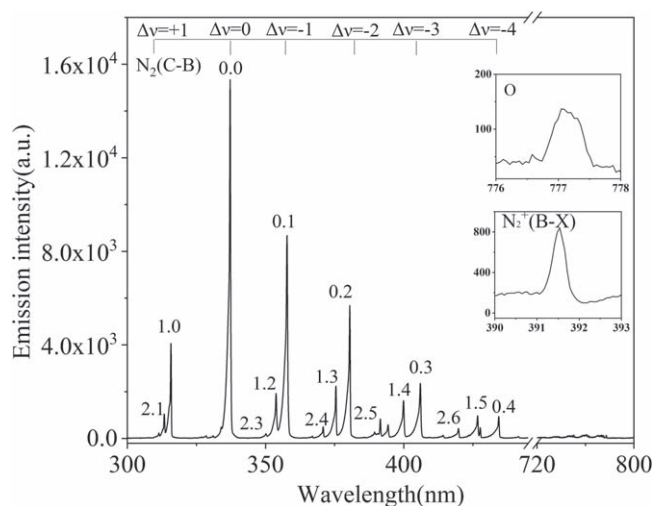


Figure 5. Emission spectrogram of the PBR.

### 3.3. The emission spectrum of the PBR

Figure 5 shows the emission spectra of the discharges in nitrogen and oxygen from 300 to 800 nm in the PBR for a discharge voltage of 25 kV, gas flow rate of  $11 \text{ min}^{-1}$ , oxygen ratio of 1% and discharge frequency of 14 kHz. It is apparent from the emission spectrum that the peak value of  $\text{N}_2(\text{C}^3\Pi_u \rightarrow \text{B}^3\Pi_g)$  at 337.1 nm is absolutely dominant in intensity and  $\text{N}_2^+(\text{B}^2\Sigma_u^+ \rightarrow \text{X}^2\Sigma_g^+)$  can also be observed at 391.4 nm. These excited nitrogen molecules can combine with oxygen molecules to form secondary reactive radicals which are effective in damaging the TIA molecules. In addition, there is a lower peak, O ( $3p^5P \rightarrow 3s^5S^0$ ), at 777 nm. Figure 6 shows the effect of applied voltage on the emission intensity of  $\text{N}_2(\text{C}^3\Pi_u \rightarrow \text{B}^3\Pi_g)$ ,  $\text{N}_2^+(\text{B}^2\Sigma_u^+ \rightarrow \text{X}^2\Sigma_g^+)$  and O ( $3p^5P \rightarrow 3s^5S^0$ ) under different discharge voltages. The emission intensity becomes stronger as the applied voltage increases. The reason for this is that a higher voltage means greater kinetic energy, allowing more collisions between molecules. As the discharge voltage of the electrode gap increases, the frequency of collisions between high-energy electrons and ground-state molecules increases, resulting in an increase in the concentration of active materials. A noticeable intensity trend was also observed for the spectral intensity of  $\text{N}_2(\text{C}^3\Pi_u \rightarrow \text{B}^3\Pi_g)$ . The existence of high-energy electrons implies a higher concentration of reactive species and more interactions among particles.

### 3.4. The effect of applied voltage on the degradation of TIA

During the discharge process, the applied voltage directly affects the number and intensity of physical and chemical effects such as active substances, high-energy electrons and ultraviolet light in the plasma [16]. Therefore, the voltage can affect the efficiency of TIA degradation as well as the catalytic activity of  $\text{TiO}_2$ . As shown in figure 7, with increase in the applied voltage, the degradation efficiency from 23 to 26 kV shows an obvious upward trend, but after reaching 28 kV the growth tends to flatten. The degradation efficiency at 25 kV with added catalyst

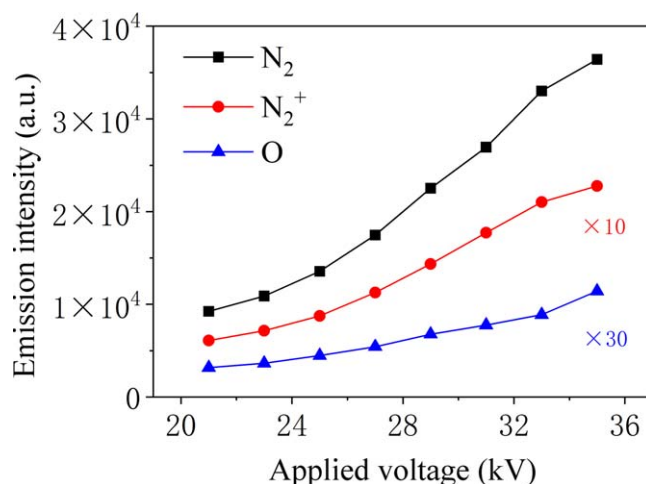


Figure 6. The intensity of  $\text{N}_2$ ,  $\text{N}_2^+$  and O varies with the applied voltage.

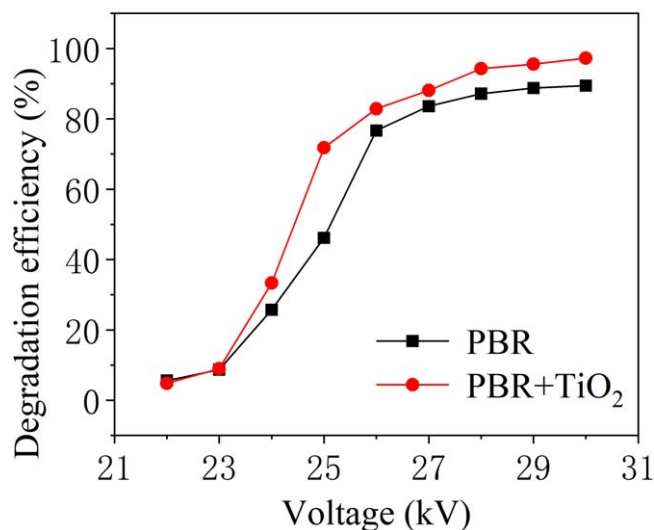
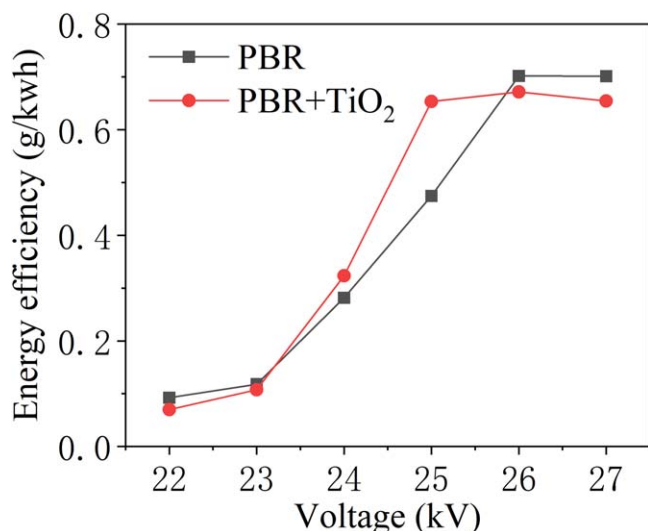


Figure 7. Effect of discharge voltage on TIA degradation efficiency.

is 25% higher than that without catalyst. Plasma and catalyst show a good synergistic effect. For an applied voltage of 30 kV, a gas flow rate of  $11 \text{ min}^{-1}$  and an oxygen ratio of 1%, treatment with the PBR combined with  $\text{TiO}_2$  catalyst for 5 min can achieve a TIA degradation efficiency of 97%.

With or without  $\text{TiO}_2$ , the energy efficiency of TIA degradation at different voltages is analyzed under the same experimental conditions in figure 8. This shows an increasing trend from 22 kV which peaks at 26 kV. Then, a downward trend is observed with increase in the discharge voltage. When the applied voltage is 25 kV, the energy efficiency of PBR for TIA degradation is 0.46, and that of PBR combined with  $\text{TiO}_2$  is 0.63. The latter displayed a distinct advantage in enhancing degradation. This is because as the discharge voltage increases more active substances are produced, but the number of TIA molecules in these regions did not change, resulting in decreased utilization of active materials. At the same time, with an increase in injected energy, more energy is used to form discharge by-products such as  $\text{O}_2$  and  $\text{NO}_x$  as well as a large amount of light and heat. In addition, from the



**Figure 8.** Variation of the energy efficiency of TIA degradation with applied voltage.

analysis of the kinetic constants of the degradation process shown in figure 9, when the applied voltage is 25 kV, the first-order reaction kinetic constants for the PBR system degrading TIA with and without TiO<sub>2</sub> are 0.25 min<sup>-1</sup> and 0.12 min<sup>-1</sup>, respectively. It is evident that in the high-voltage region, the reaction rate with the addition of catalyst has obvious advantages. This is because a higher applied voltage realized an improved activity and stability of the TiO<sub>2</sub> catalyst [17]. At the same time, the UV light and heat generated during the discharge can also directly act on the TIA molecules and the TiO<sub>2</sub> catalyst to enhance the degradation effect [18].

### 3.5. The effect of treatment time on degradation efficiency

The effect of treatment time on TIA degradation efficiency by DBD with and without TiO<sub>2</sub> is shown in figure 10. The experimental conditions are as follows: applied voltage 25 kV, gas flow rate 1 l min<sup>-1</sup> and oxygen ratio 1%. It can be seen from the experimental curve that the concentration of TIA decreases as the time of discharge treatment increases. When the treatment time was only 5 min, the efficiency of TIA degradation in PBR and PBR + TiO<sub>2</sub> reached 46.3% and 76.8%, respectively. However, the efficiency of TIA degradation increased to 90.7% and 95.2% when the treatment time was increased to 13 min. The experimental results show that the addition of catalyst can effectively improve the efficiency of TIA degradation in a short time. However, as the treatment time increases and energy continues to be injected, the number of TIA molecules gradually decreases the trend of increasing degradation gradually slows.

### 3.6. The effect of gas flow rate on the degradation of TIA

To investigate the effects of gas flow rate on the degradation of TIA, the reactions were conducted for various conditions of gas flow rate, but under the same degradation conditions, and compared with the catalyst-added reactions in figure 11. The working gases are nitrogen and oxygen, and the applied voltage is 25 kV, the oxygen ratio is 1%, and the treatment time is 5 min.

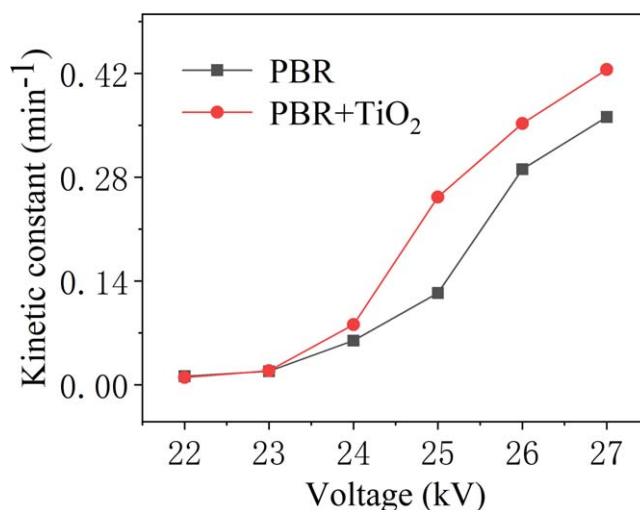


**Figure 9.** Variation of the kinetic constant of TIA degradation with applied voltage.

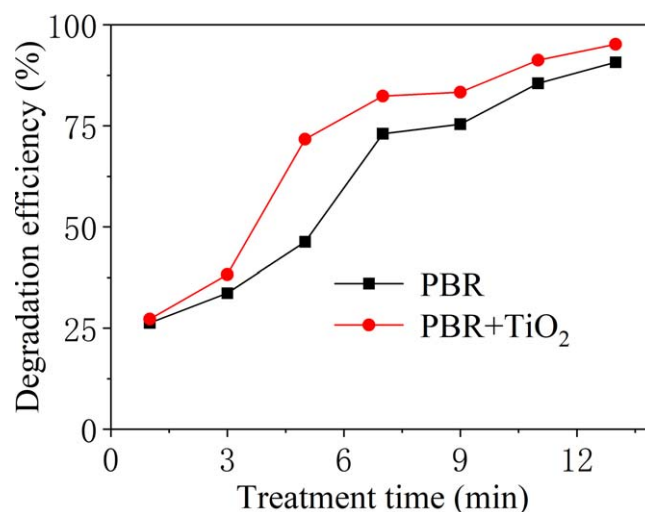


**Figure 10.** Variation of degradation efficiency with treatment time.

Apparently, the gas flow rate strongly influences the removal efficiency. With increase in the gas flow rate, the efficiency of TIA degradation first increases and then decreases significantly. When the gas flow rate is 0.6 l min<sup>-1</sup>, the TIA degradation efficiency of PBR combined catalyst can reach 78.6%, which is 18.4% higher than that of PBR alone. The higher degradation efficiency would depend on increasing the amount of active material generated in the discharge area per unit area per unit time with increase in the initial gas flow. However, a continued rise in the gas flow rate leads directly to a decreased in the residence time, resulting in a reduced number of collisions between active particles and TIA molecules, thus reducing the degradation of TIA.

### 3.7. The effect of oxygen concentration on the degradation of TIA

Figure 12 shows the effect of oxygen concentration on the efficiency of TIA degradation for an applied voltage of 25 kV, gas flow rate of 0.6 l min<sup>-1</sup>, discharge frequency of 14 kHz and

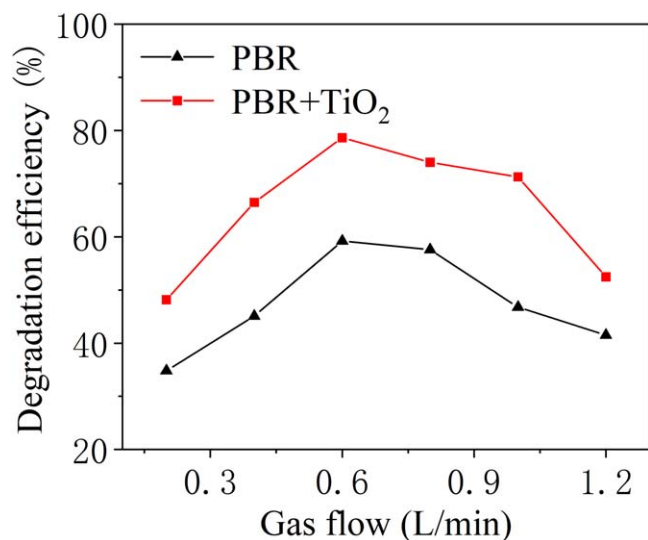


**Figure 11.** The effect of gas flow rate on efficiency of TIA degradation.

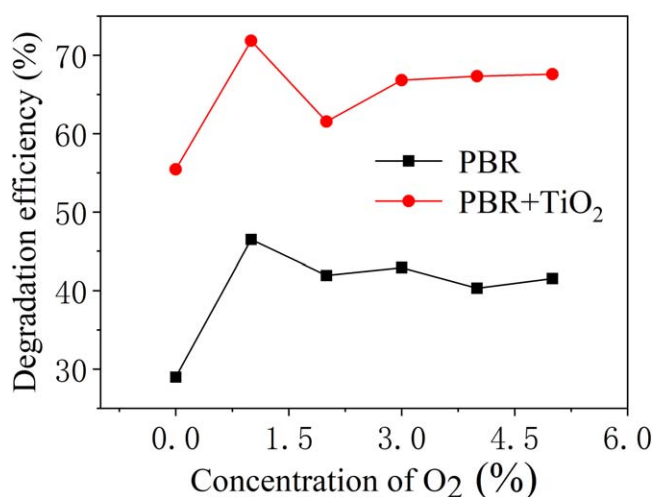


**Figure 12.** Effect of the oxygen concentration on the efficiency of TIA degradation.

treatment time of 5 min. This treatment was carried out under the same degradation conditions and compared with the results with the addition of catalyst. It can be seen that a higher TIA degradation efficiency was achieved in the presence of TiO<sub>2</sub> catalyst. The change in the oxygen concentration affected the efficiency of TIA degradation, and the trend of the graph resembles the curve of the catalyst-added results. When the oxygen ratio is 1%, the degradation efficiency of the sample with added catalyst reaches 71.9% compared with 45.5% without the catalyst, these being the respective peak values. However, when the proportion of oxygen is greater than 1%, the efficiency of TIA degradation decreases significantly with increase in the oxygen concentration. The addition of oxygen to nitrogen plasma may produce more gaseous reactive oxygen species and may also reduce the intensity of plasma as it is an electronegative gas. When the oxygen ratio is too high, it consumes a large number of high-energy electrons and reduces the density of high-energy electrons in the discharge zone. On the

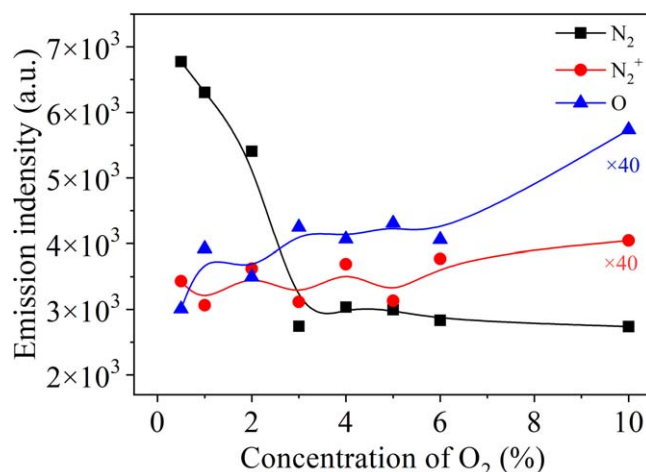


**Figure 13.** Variation in the intensity of N<sub>2</sub>, N<sub>2</sub><sup>+</sup> and O with the concentration of oxygen.

other hand, the increase in reactive oxygen species will lead to a decrease in active nitrogen, because some oxygen active substances can react with nitrogen active substances and this is not conducive to the degradation of TIA.

The difference in oxygen content in the working gas can significantly affect the occurrence of chemical reactions and the production of active materials during the discharge process. Figure 13 shows how the intensity of emission of N<sub>2</sub> ( $C^3\Pi_u \rightarrow B^3\Pi_g$ ), N<sub>2</sub><sup>+</sup> ( $B^2\Sigma_u^+ \rightarrow X^2\Sigma_g^+$ ) and O ( $3p^5P \rightarrow 3s^5S^0$ ) changes as the oxygen concentration changes under the same experimental conditions. When the oxygen ratio increases from 1% to 10%, the spectral intensities shows different trends. When the oxygen ratio is 1%, N<sub>2</sub> ( $C^3\Pi_u \rightarrow B^3\Pi_g$ ) is dominant in the spectrum, but as the oxygen ratio continues to increase, the intensity of N<sub>2</sub> ( $C^3\Pi_u \rightarrow B^3\Pi_g$ ) decreases sharply. Its decline decreases with further increase in the oxygen content. The emission spectral intensity of N<sub>2</sub><sup>+</sup> ( $B^2\Sigma_u^+ \rightarrow X^2\Sigma_g^+$ ) shows no obvious change with increase in the oxygen content. The intensity of O ( $3p^5P \rightarrow 3s^5S^0$ ) does not change significantly for increase in the oxygen content from 1% to 8%, but gradually rises as the oxygen content increases from 8% to 10%. This is due to the increased oxygen content in the working gas as the nitrogen content decreases: the nitrogen-containing active substances that can react with oxygen decrease, so that the O( $3p^5P \rightarrow 3s^5S^0$ ) content gradually increases. At the same time, because the increase in oxygen content consumes more electrons, which leads to the weakening of collisions, dissociation and excitation caused by high-energy electrons, the intensity of N<sub>2</sub> ( $C^3\Pi_u \rightarrow B^3\Pi_g$ ) decreases sharply. N<sub>2</sub><sup>+</sup> itself is weak: although it also has a decreasing trend with increase in the oxygen content the change is not obvious.

#### 4. Exploration of the degradation mechanism

The effects of discharge plasma on pollutants are mainly three-fold. On the one hand, high-energy electrons have huge energy that can directly impact and destroy the chemical bonds of

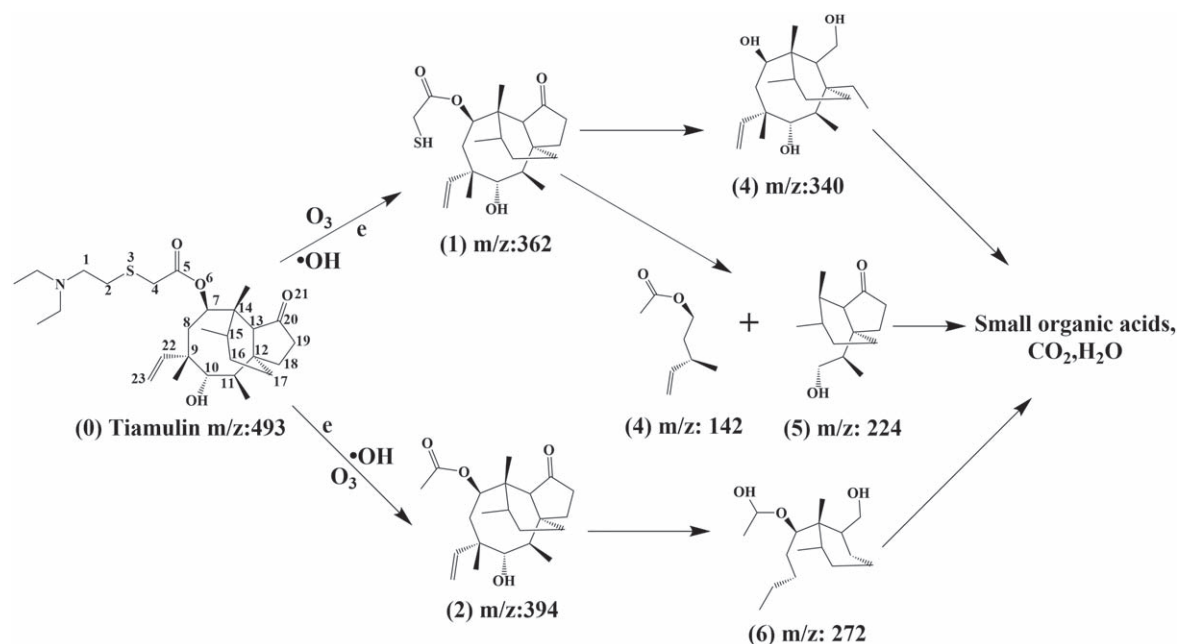
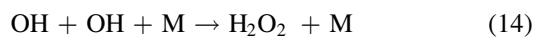
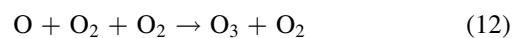
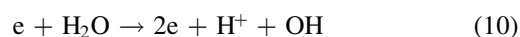
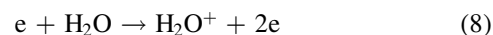
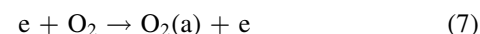
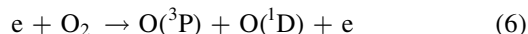
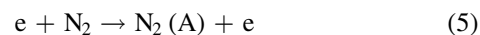


Figure 14. Derivation of possible pathways for TIA degradation.

pollutant molecules, breaking them and achieving the effect of decomposition. On the other hand, high-energy electrons can also react with molecules in the working gas. The generated O, OH, O<sub>3</sub>, N and N<sub>2</sub>(A<sup>3</sup>Σ<sub>u</sub><sup>+</sup>) and other active substances act on pollutant molecules to oxidize and degrade them [19]. In parallel, UV produced by the discharge process may directly generate free radicals, responsible for the generation of reactive oxygen species, through photochemical reaction because UV photons have sufficient energy to destroy chemical bonds [20]. When plasma acts on TIA molecules, C–H bonds (bond energy 4.3 eV) are more likely to be attacked by high-energy electrons, high-energy excited molecules and active substances than C–C bonds (bond energy 5.5 eV) to cause cleavage [21]. The oxidation of active groups is the main reason for further degradation of TIA molecules.

The experimental results show that the degradation efficiency for the sample with added TiO<sub>2</sub> catalyst is significantly higher than that for the sample without catalyst under the same experimental conditions, indicating that TiO<sub>2</sub> is excited to generate electron–hole pairs under plasma discharge, thereby producing more active materials. Whitehead and others believe that high-energy electrons are the main reason for the stimulation of TiO<sub>2</sub> to produce electron–hole pairs. At the same time, in the plasma discharge process gas molecules are ionized and excited under the action of a strong electric field. When the excited particles produced by ionization recombine or transition from the excited state to a lower energy level or ground state, a large amount of light energy radiates out, which also stimulates TiO<sub>2</sub> to generate electron–hole pairs [22]. Specifically, the working gas generally contains a small amount of moisture and various trace gases in addition to oxygen and nitrogen. After excitation of the electron–hole pairs on the TiO<sub>2</sub> attached to the surface of particles, the photon-generated electrons will react with oxygen in the water to form superoxide anion radicals, which interact with hydrogen peroxide

and molecular oxygen species. At the same time, the holes will react with hydroxyl groups in the water to form hydroxyl radicals. Banaschik *et al* treated seven refractory drugs by a pulse plasma method. They studied the degradation kinetics and degradation pathways of dichlorobenzoic acid in detail and confirmed the important role of hydroxyl radicals and hydrogen peroxide in the decomposition of diclofenac [23]. The main reaction mechanisms of the plasma catalyst system are as follows [24–26]:



Spectroscopic and high-performance liquid chromatography–mass spectrometry (HPLC-MS) analyses were applied to analyze the feasible pathway for removal of TIA. The molecular formula of TIA is C<sub>28</sub>H<sub>47</sub>NO<sub>4</sub>S (*m/z*: 493), and it belongs to the class of macrolide antibiotics. Figure 14 proposes three possible reaction pathways for the reaction (numbers in brackets refer to the labeled processes in the figure). The molecular bonds of TIA are first bombarded by high-energy electrons. Due to the low bond energy (272 kJ mol<sup>−1</sup>), the S–C bonds break first [27]. Under the action of active particles and excited molecules,



including energetic electrons, neutral and excited molecules/atoms, (1) ( $m/z$ : 362) is produced by C–S bond breaking between  $C_2$  and  $S_3$ . Similarly, (2) ( $m/z$ : 394) is also formed by the rupture of the C–S bond between  $C_4$  and  $S_3$ . The esterification and reduction reaction of  $C_5C_6$  and the oxidation–reduction reaction of ketone at  $C_{20}$  cause the rupture of  $C_{19}$  and  $C_{20}$  to form (3) ( $m/z$ : 340). The active particles in the solution release the ring tension of the eight-membered ring and break the C–C bond between  $C_7$  and  $C_{14}$ ,  $C_{11}$  and  $C_{12}$ , forming (4) ( $m/z$ : 142) and (5) ( $m/z$ : 224). The C–S bonds continue to break and the C–C bonds between  $C_9$  and  $C_{10}$  and between  $C_{11}$  and  $C_{12}$  are broken with the opening of the eight-membered ring. After the opening of the five-membered ring, the side base of the short chain is removed and forms (6) ( $m/z$ : 272). With further interaction of these particles with the active oxidation groups, (3), (4), (5) and (6) are further degraded into small organic acids,  $CO_2$  and  $H_2O$ . The pathway of TIA

degradation deduced above is clearly supported by the HPLC-MS results in figure 15.

According to the characteristics of the TIA molecule and its interaction with high-energy electrons and active particles, the potential energy profile (PES) was calculated for the degradation path deduced above. This verified our speculations about the possible degradation path (figure 16).

## 5. Conclusion

In this study, plasma generated from the discharge of a packed bed dielectric barrier (PBR) reactor driven by an AC power supply was used to degrade the solid-phase antibiotic TIA loaded on simulated soil particles. The initial concentration of the solution selected for soaking the sample was  $4\text{ g l}^{-1}$ , and the supernatant concentration of the sample after adsorption and desorption was  $216.163\text{ mg l}^{-1}$ . When nitrogen and oxygen are used as the working gases, the PBR reactor can produce an effective large-area discharge. The spectra exhibit three well-resolved emission bands,  $N_2(C^3\Pi_u \rightarrow B^3\Pi_g, 340\text{ nm})$ ,  $N_2^+(B^2\Sigma_u^+ \rightarrow X^2\Sigma_g^+, 394.1\text{ nm})$  and  $O(3p^5P \rightarrow 3s^5S^0, 777\text{ nm})$ , the emission intensity of which was enhanced with increasing applied voltage. The effects of applied voltage, discharge time, oxygen ratio, gas flow rate and catalyst on the efficiency of degradation of TIA were investigated. The findings showed that plasma and catalyst can produce a synergistic effect: when applied voltage is 25 kV, the oxygen ratio is 1%, the gas flow rate is  $0.6\text{ l min}^{-1}$  and the treatment time is 5 min, the degradation efficiency of plasma combined with catalyst can reach 78.6%, which is 18.4% higher than that of plasma without catalyst. It can be concluded that the higher applied voltage and longer processing

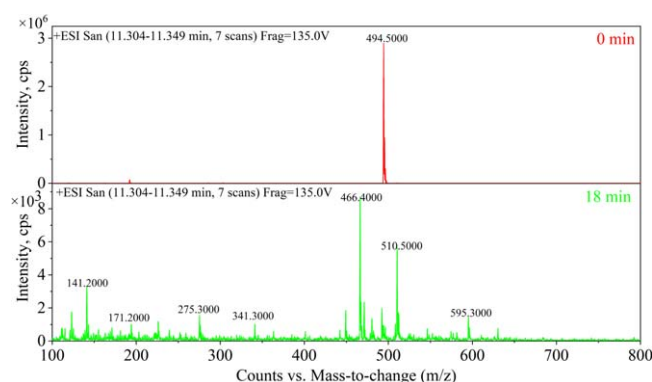


Figure 15. HPLC-MS for TIA degradation.

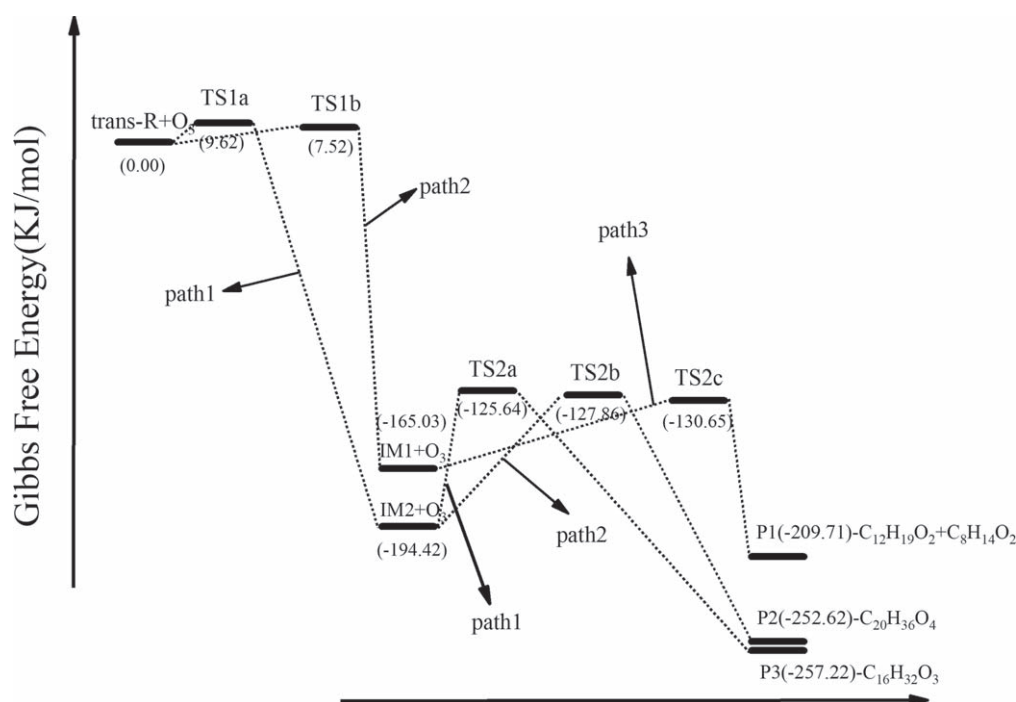


Figure 16. Profile of the potential energies of the reaction products.

time lead to more degradation, but also result in a lower energy efficiency. When the oxygen ratio is 1%, the degradation efficiency for the sample with the catalyst added reaches 71.9% while that for the sample without catalyst is 45.5%, both being the respective peak values). When the oxygen ratio is too high, the oxygen consumes a large number of high-energy electrons and reduces the density of high-energy electrons in the discharge zone. Plasma combined catalyst has many effects on pollutants. Active substances formed by combined catalytic discharge are highly reactive, including many high-energy electrons, free radicals, ions and excited molecules and atoms, which play a key role in the degradation of TIA. The ring of the TIA molecule is opened under the continuous action of high-energy electrons and active substances and continues to open and degrade to small molecular organic acids, CO<sub>2</sub>, and H<sub>2</sub>O. Combined with mass spectrometry and potential energy calculations, we demonstrate the feasibility of the deduced degradation pathway.

### Acknowledgments

This work is supported by National Natural Science Foundation of China (Nos. 51967018, 11965018 and 51967017), the Science and Technology Development Fund of Xinjiang Production and Construction (No. 2019BC009) and the Innovation and Development Special Project of Shihezi University (No. CXFZ202105).

### References

- [1] An J et al 2015 *Environ. Earth Sci.* **74** 5077
- [2] Shi H M et al 2020 *Environ. Chem. Lett.* **18** 345
- [3] Sodhi K K et al 2021 *SN Appl. Sci.* **3** 269
- [4] Lee D et al 2018 *Chemosphere* **209** 901
- [5] Zheng C H et al 2014 *J. Ind. Eng. Chem.* **20** 2761
- [6] Kim K S, Yang C S and Mok Y S 2013 *Chem. Eng. J.* **219** 19
- [7] Guo H et al 2019 *Chemosphere* **230** 190
- [8] Aziz K H H et al 2017 *Chem. Eng. J.* **313** 1033
- [9] He D et al 2014 *Chem. Eng. J.* **258** 18
- [10] Zhou Z Y et al 2017 *Chem. Eng. Process.: Process Intensif.* **115** 23
- [11] Li J et al 2011 *Plasma Sources Sci. Technol.* **20** 034019
- [12] Ma T J and Xu Y Q 2013 *Adv. Mater. Res.* **781–784** 1637
- [13] Borak M D et al 2020 *Clin. Toxicol.* **58** 287
- [14] Jiang B et al 2014 *Chem. Eng. J.* **236** 348
- [15] Scholtz V et al 2015 *Biotechnol. Adv.* **33** 1108
- [16] Tang S F et al 2018 *Chem. Eng. J.* **337** 446
- [17] Zhao W F et al 2020 *J. Environ. Chem. Eng.* **8** 102206
- [18] Wang Y H et al 2017 *J. Photochem. Photobiol. A* **342** 94
- [19] Hu J et al 2016 *Chem. Eng. J.* **293** 216
- [20] Sang W J et al 2019 *Chemosphere* **236** 124401
- [21] Sarangapani C et al 2019 *Sci Rep.* **9** 3955
- [22] Wang L et al 2018 *Plasma Process. Polym.* **15** 1700176
- [23] Lukes P et al 2005 *Res. Chem. Intermed.* **31** 285
- [24] Sohrabi A et al 2019 *Desalin. Water Treat.* **139** 202
- [25] Sokolov A et al 2018 *Chem. Eng. J.* **334** 673
- [26] Zhang G Y et al 2017 *J. Hazard. Mater.* **323** 719
- [27] Zhang Q F et al 2018 *Chemosphere* **210** 433